Volcanic and tectonic deformation on Unimak Island in the Aleutian Arc, Alaska

Dörte Mann[1] and Jeffrey Freymueller
Geophysical Institute, University of Alaska, Fairbanks, Alaska, USA

Received 13 April 2002; revised 31 August 2002; accepted 17 October 2002; published 20 February 2003.

[1] GPS measurements on Unimak Island in the eastern Aleutian arc between 1998 and 2001 show deformation of Westdahl volcano and Fisher caldera. Westdahl is inflating, with the best fit point source located at $7.2^{+2.3}_{-1.2}$ km depth and a volume change rate of $6.7^{+3.3}_{-1.8} \times 10^6$ m^3 yr^{-1}. The GPS data indicate that inflation may have slowed down slightly compared with interferometric synthetic aperture radar (InSAR) observations between 1993 and 1998. The accumulated subsurface volume increase during the GPS and InSAR observation period (1993–2001), $\sim 70 \times 10^6$ m^3, already accounts for at least 15% more than the erupted volume from the last eruption in 1991–1992. Fisher caldera shows subsidence and contraction across the caldera center. The data are fit best with a rectangular dislocation source at a shallow depth. It is 14 km long and 0.5 km wide, dips 80° to the NW, and strikes N35°E, with rather large uncertainties for most of these parameters. Its volume decrease is 2.0×10^6 m^{3}yr^{-1}. The main mechanisms to explain the subsidence and contraction are degassing and contractional cooling of a shallow magma body and depressurization of Fisher's hydrothermal system, possibly triggered by an earthquake in 1999. At the 95% confidence level, no significant strain accumulation due to subduction is observed across the entire island. The low coupling across the rupture zone of the 1946 earthquake is a strong argument for the idea that the earthquake and tsunami did not result from a purely double-couple (earthquake) source. *INDEX TERMS:* 1206 Geodesy and Gravity: Crustal movements—interplate (8155); 8135 Tectonophysics: Evolution of the Earth: Hydrothermal systems (8424); 8145 Tectonophysics: Evolution of the Earth: Physics of magma and magma bodies; 8150 Tectonophysics: Evolution of the Earth: Plate boundary—general (3040); *KEYWORDS:* volcanic deformation, caldera deformation, Aleutian Arc, Alaska, Unimak Island

Citation: Mann, D., and J. Freymueller, Volcanic and tectonic deformation on Unimak Island in the Aleutian Arc, Alaska, *J. Geophys. Res.*, *108*(B2), 2108, doi:10.1029/2002JB001925, 2003.

1. Introduction

[2] The Alaska-Aleutian arc represents a highly active tectonic and volcanic environment, driven by subduction of the Pacific plate underneath the North American plate. In historical time (since 1760), at least 29 volcanic centers along the arc have erupted more than 265 times [*Miller et al.*, 1998]. Since 1938, nearly all segments of the arc have ruptured in at least one $M > 7.5$ earthquake.

[3] The central part of the arc (Figure 1) is of particular interest for its volcanic as well as tectonic features. Volcanoes are spaced ~40 km apart, but despite this closeness, they have quite different physical appearances, seismicity, and eruption behaviors. Two of the volcanoes on Unimak Island, Westdahl and Shishaldin (Figure 1), have erupted within the past 10 years. Westdahl erupted in 1991/1992, producing a basaltic lavaflow down its northeast flank [*Miller et al.*, 1998]. The volume of the flow was ~30–60 $\times 10^6$ m^3 [*Rowland et al.*, 1994]. Interferometric synthetic aperture radar (InSAR) has shown that Westdahl has been inflating since then, at possibly variable rates [*Lu et al.*, 2000a]. The Alaska Volcano Observatory (AVO) installed a seismic network around Westdahl in 1998 but has yet to register any significant earthquakes under the volcano. Between Westdahl and Shishaldin lies Fisher, a large Holocene caldera that was formed approximately 9100 years ago [*Miller et al.*, 1998]. Although Fisher has been much less active than either Shishaldin or Westdahl in recent times, it shows high hydrothermal activity.

[4] Subduction processes in this area of the arc are not laterally uniform. To the east, in the western Shumagin segment, GPS measurements show that no strain is accumulating, indicating that the plates are not coupled and the Pacific plate is slipping freely underneath the North American plate [*Freymueller and Beavan*, 1999]. The situation is less certain to the west. The rupture zone of the 1957 M_W 9.1 earthquake extends from the western end of Unimak Island westward to the Andreanof Islands [*Kanamori*, 1977]. This could indicate strong coupling between the North American and the Pacific plates, which would cause contraction across the arc and forearc during the interseismic period. Other

[1]Now at Department of Geophysics, Stanford University, Stanford, California, USA.

0148-0227/03/2002JB001925$09.00

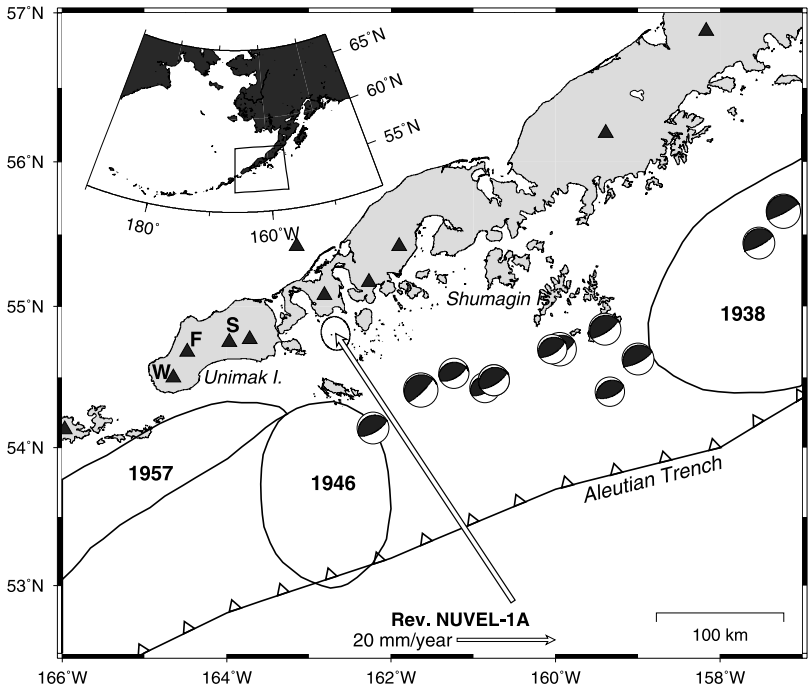

Figure 1. Location map and tectonic setting of the central Aleutian arc and Unimak Island. Aftershock zones and dates of major earthquakes are indicated. Focal mechanisms are from the Harvard CMT catalog, based on events with $M_W > 6.0$. The arrow shows the revised NUVEL-1A Pacific-North America relative motion. Historically active volcanoes are shown as dark triangles. W is Westdahl, F is Fisher, and S is Shishaldin.

studies [e.g., *Johnson and Satake*, 1993] show evidence that the western Unimak area did not rupture during the 1957 earthquake. The 1946 M_S 7.4 earthquake may have ruptured a section of the megathrust offshore Unimak Island. This earthquake is notable because it generated a disproportionately large tsunami given its surface wave magnitude (tsunami magnitude, M_t, 9.3 [*Abe*, 1979]). This earthquake has been modeled as both a single couple source (landslide), as well as a standard double couple earthquake source. *Kanamori* [1985] preferred a landslide source, while several others have argued in favor of an earthquake source [*Davies et al.*, 1981; *Okal*, 1988; *Pelayo*, 1990; *Johnson and Satake*, 1997]. Recently, *Fryer et al.* [2002] cited bathymetric evidence for the landslide source and suggested that a large landslide triggered by a small earthquake caused the tsunami, and the source process of the 1946 earthquake and tsunami is once again under debate.

[5] Geodetic observations have a relatively short history in the Aleutians, but have proven increasingly useful to detect volcanic unrest, learn about characteristics specific to individual volcanoes, and determine the principal tectonic mechanisms. In this paper, we analyze GPS data from Unimak Island acquired between 1998 and 2001 and interpret the observed deformation in terms of volcanic and tectonic activities. We focus on the deformation of Westdahl and Fisher volcanoes and the plate coupling in the source region of the 1946 earthquake.

2. GPS Data

[6] Measurement of the GPS network on Unimak Island volcanoes (Figure 2) began in 1998. Observations were made at 5 stations around Westdahl volcano. In 1999, these stations were reoccupied, and seven new stations were established, five of them in neighboring Fisher caldera. In 2000, all stations except FC03 and in 2001 all stations in Fisher caldera and several on Westdahl were resurveyed. Most surveys lasted for one or more 24-hour session, but in some cases, time limitations allowed only a short (several hour) occupation. Stations KATY and PANK at the east end of the island have a longer observation history, going back to 1993 and 1995, respectively. KATY served as reference station during all recent campaigns, and PANK was resurveyed during the last campaign in 2001.

[7] The GIPSY software [*Zumberge et al.*, 1997] was used to analyze the GPS data. Daily solutions were transformed to the ITRF97 reference frame [*Boucher et al.*, 1999], and combined to estimate site velocities. Details of our analysis methods are given by *Freymueller et al.* [1999, 2000]. To obtain velocities relative to the North American plate (NOAM), we used the pole and rotation for the ITRF97-NOAM relative motion given by *Sella et al.* [2002]. Uncertainties in the estimated velocities are scaled such that the reduced χ^2 statistic of the velocity solution equals 1.0. Typical uncertainties in the horizontal components are 1–2 mm yr^{-1}. Uncertainties in the vertical component are larger, generally 4–6 mm yr^{-1}. We use both horizontal and vertical GPS velocities, weighted by their covariances, for the data inversion.

[8] To investigate deformation on the island, we compute velocities relative to station KATY (Table 1 and Figure 2). Because of its location, KATY is presumably not influenced by volcanic deformation, nor does it experience strain

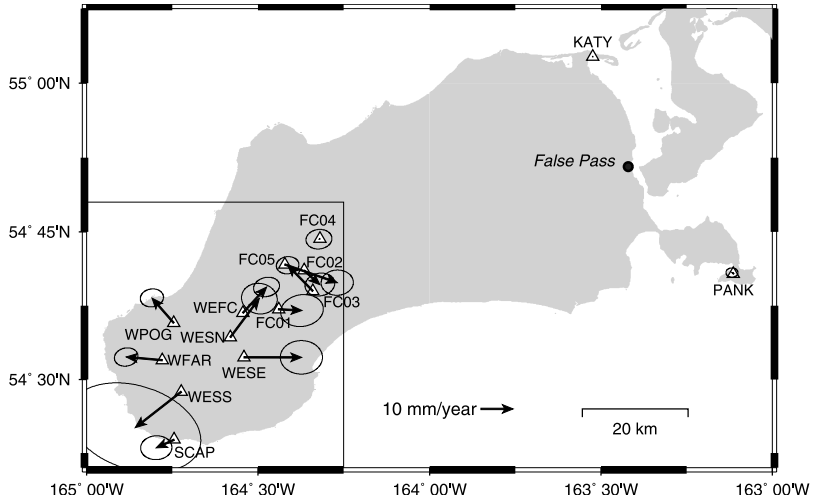

Figure 2. GPS sites and horizontal velocities on Unimak Island between 1998 and 2001. Velocities are relative to site KATY at the northeast end of the island. Velocity at PANK includes a survey from 1997, velocity at KATY also includes surveys from 1993, 1995, and 1997. Error ellipses indicate 95% confidence regions. The data show outward radial displacement at Westdahl volcano, and contraction across the caldera floor at Fisher. The box outlines the area shown in Figure 3. False Pass is a small fishing village and the only community on the island.

accumulation resulting from subduction [*Freymueller and Beavan*, 1999]. This is supported by our new data which show that station PANK does not move relative to KATY (Figure 2). Relative to North America, KATY moves 4.0 ± 0.5 mm yr^{-1} oriented toward N214 ± 8°E, and PANK and other sites along the Alaska Peninsula immediately to the east show similar velocities [*Freymueller and Beavan*, 1999].

[9] On Unimak Island, the data show general uplift and outward radial displacement at Westdahl volcano and subsidence and contraction across the caldera floor at Fisher. There is no obvious signal caused by a locked subduction interface, except perhaps at Scotch Cap (SCAP) (Figure 2). All velocites are averaged over the whole observation period (3 years at Westdahl, 2 years at Fisher), because most sites have too few occupations to construct a more detailed time series.

3. Models

[10] We model the GPS data in terms of volcanic and tectonic deformation, using an elastic half-space model. On the basis of the radial deformation pattern and previous modeling work by *Lu et al.* [2000a], we assume a pressure point source [*Mogi*, 1958] underneath Westdahl volcano. For Fisher, we investigate a variety of models: a Mogi point source like the one used at Westdahl, a rectangular dislocation source [*Okada*, 1985], and a finite ellipsoidal pressure source [*Yang et al.*, 1988]. Strain accumulation across the subduction boundary is modeled using dislocation theory as virtual normal slip on the locked part of the plate interface [*Savage*, 1983].

[11] We use a random cost algorithm [*Berg*, 1993] to invert all three components of the GPS data. We apply a bootstrap method to estimate 95% confidence intervals for the model parameters. For a detailed discussion of the methods and their applications to geodetic data, see *Cervelli et al.* [2001]. In a first model run, we jointly invert for two volcanic sources, modeling a full set of parameters, four for the point source, and eight for either the dislocation or the finite ellipsoidal source. In a second run, we include strain accumulation due to subduction at the west end of Unimak Island by estimating two additional parameters, the width of the locked interface and the degree of coupling.

3.1. Volcanic Deformation

[12] From models based on InSAR observations between 1993 and 1998 [*Lu et al.*, 2000a], we could have placed some bounds on model parameters for the point source underneath Westdahl volcano. Instead, we allowed a wide range for each parameter in case there had been temporal changes in the deformation source. The best fit point source underneath Westdahl is located slightly northeast of Westdahl Peak, at 54.5°N, 164.6°W, at 7.2 km depth. The inferred subsurface volume change is $+6.7 \times 10^6$ m^3 yr^{-1}, assuming that the Mogi source strength is entirely due to volume change.

Table 1. Site Velocities Relative to KATY[a]

Site	Lat, °N	Long, °E	V_{east}, mm yr^{-1}	V_{north}, mm yr^{-1}	V_{up}, mm yr^{-1}
SCAP	54.40	−164.74	−6 ± 2	−3 ± 2	8 ± 5
WESS	54.34	−164.72	−14 ± 8	−11 ± 6	−1 ± 16
WESE	54.54	−164.54	18 ± 3	0 ± 2	−2 ± 6
WESN	54.57	−164.58	9 ± 2	12 ± 2	19 ± 6
WPOG	54.60	−164.68	−7 ± 1	8 ± 1	6 ± 4
WFAR	54.53	−164.78	−11 ± 1	1 ± 1	6 ± 4
WEFC	54.61	−164.54	7 ± 2	8 ± 1	9 ± 4
FC01	54.62	−164.44	7 ± 3	0 ± 2	−7 ± 6
FC02	54.68	−164.37	5 ± 2	−4 ± 1	−15 ± 4
FC03	54.65	−164.34	−8 ± 1	8 ± 1	−8 ± 3
FC04	54.74	−164.32	0 ± 2	0 ± 1	−3 ± 4
FC05	54.69	−164.42	16 ± 2	−6 ± 2	0 ± 5
PANK	54.68	−163.11	0 ± 1	1 ± 1	0 ± 2

[a]Uncertainties are 1σ.

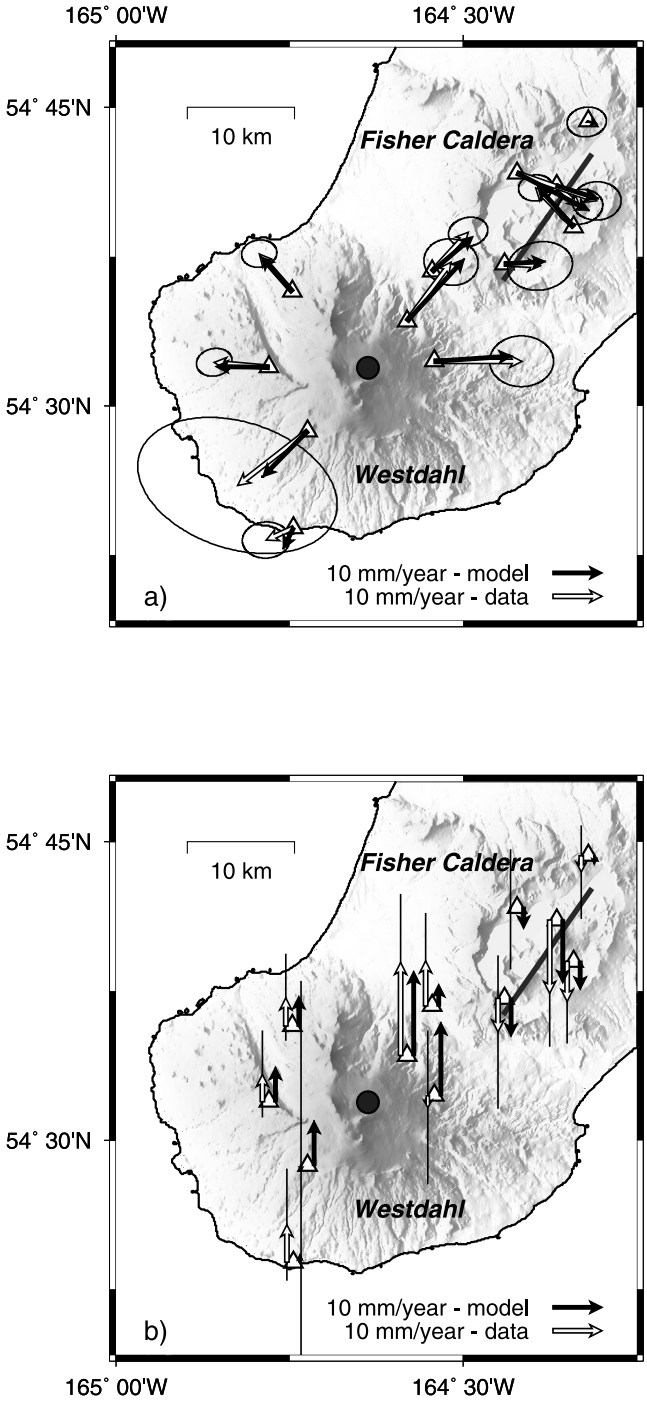

Figure 3. (a) Horizontal and (b) vertical data (open arrows) and best fit model (solid arrows) for volcanic deformation only. The solid dot on Westdahl indicates the location of the pressure point source, the solid line in Fisher indicates the location of the rectangular dislocation source.

[13] The best fit rectangular dislocation source underneath Fisher caldera is 13.7 km long and 0.5 km wide, and its upper edge is located at 1.6 km depth. The plane strikes N35°E, and it dips 80° to the NW. The amount of contraction is 0.3 m yr^{-1}. The best fit ellipsoidal pressure source has a similar location and extent as the rectangular dislocation. Its center is located at 2.1 km depth, its semimajor axis is 4 km long, the semiminor axis is 0.5 km, and the pressure change is -25 kPa yr^{-1}. The best fit Mogi source is located in the approximate center of the caldera at 3.5 km depth. It requires a subsurface volume change of -1.3×10^6 m^3 yr^{-1}.

[14] The best overall fit to the data is provided by a combination of a Mogi point source beneath Westdahl and a dislocation source beneath Fisher caldera, with a sum of squared errors (SSE) of 33.60. A combination of a Mogi source and a finite ellipsoidal source gives an SSE of 75.12, and a combination of two Mogi sources gives an SSE of 82.56. Figure 3 shows the data and velocities predicted from the best fit model combination for the two volcanic sources. Tables 2 and 3 summarize the parameters and their uncertainties for the Mogi source and the dislocation source, respectively.

[15] While all model parameters for the Mogi source underneath Westdahl, especially the source location, are well constrained, several parameters of the dislocation underneath Fisher are not. In particular, the length of the dislocation plane has large uncertainties. Depth and dip are bimodally distributed, allowing for either of two geometries: shallow and vertical, or deeper and horizontal (Figure 4a). In all best fitting models, however, the product of the contraction and the area of the dislocation remains nearly constant at 2.0×10^6 m^3 yr^{-1}.

3.2. Strain Accumulation Due to Subduction

[16] *Johnson and Satake* [1997] modeled the 1946 tsunami waveforms assuming an earthquake source, and suggested that 9–10 m of slip on a shallow fault plane 100 by 80 km in size (M_W 8.4) explained the tsunami waveforms. Such a large amount of slip is similar to that observed in 1964 in the Kodiak asperity, the smaller asperity that ruptured in the 1964 Alaska earthquake [*Johnson et al.*, 1996]. If such a large amount of slip occurred in the 1946 earthquake, we would expect to find geodetic evidence for a large locked patch offshore of Unimak Island, similar to the large locked patches that correspond to the two 1964 earthquake asperities [*Zweck et al.*, 2002]. Such a locked patch would cause significant strain across Unimak Island and motion of sites in the direction of relative plate motion. Conversely, the lack of such strain and that component of velocity would argue in favor of the landslide source for the 1946 earthquake.

[17] *Freymueller and Beavan* [1999] showed that there is no strain accumulation in the western Shumagin segment of the arc, which lies at the eastern boundary of our study area. This results from free slip on the plate interface due to weak frictional coupling. Our reference station KATY is within this free-slip area (Figure 1). Because station FC04 shows no movement relative to KATY (Figure 2), we assume that deformation in Fisher caldera is not affected by subduction-

Table 2. Point Source Parameters[a]

Lat, °N ± km	Long, °E ± km	Depth, km	ΔVolume, $\times 10^6$ m^3 yr^{-1}
$54.532^{+1.6}_{-1.2}$	$-164.637^{+1.2}_{-1.3}$	$7.2^{+2.3}_{-1.2}$	$6.7^{+3.3}_{-1.8}$
$54.535^{+1.4}_{-1.3}$	$-164.633^{+1.0}_{-1.5}$	$7.3^{+2.4}_{-1.3}$	$6.7^{+3.3}_{-1.8}$

[a]First row gives results when only volcanic sources are estimated, and the second row gives the best estimates when both volcanic and tectonic sources are estimated. Uncertainties show 95% confidence.

Table 3. Rectangular Dislocation Source Parameters

Length, km	Width, km	Depth, km	Dip, deg	Strike, N°E	Closure, m	Lat, °N ± km	Long, °N ± km
$13.7^{+4.1}_{-10.5}$	$0.5^{+2.0}_{-0.3}$	$1.6^{+2.6}_{-1.4}$	80^{+51}_{-58}	35^{+23}_{-28}	$0.32^{+0.67}_{-0.21}$	$54.658^{+3.5}_{-2.3}$	$-164.379^{+3.2}_{-3.3}$
$12.1^{+5.7}_{-8.9}$	$0.5^{+3.9}_{-0.3}$	$1.7^{+2.7}_{-1.4}$	82^{+48}_{-79}	36^{+29}_{-29}	$0.38^{+0.61}_{-0.27}$	$54.652^{+3.5}_{-1.2}$	$-164.384^{+2.2}_{-1.5}$

First row are results when only volcanic sources are estimated, the second row are the best estimates when both volcanic and tectonic sources are estimated. Uncertainties show 95% confidence.

related strain accumulation either. A fully locked subduction zone offshore of this part of Unimak Island would produce ~10 mm yr^{-1} of motion of FC04 relative to KATY, so we can clearly rule out this possibility. At Westdahl, only one station (SCAP) shows displacements that deviate from the radial pattern around the volcano. We thus assume that only SCAP and the stations closest to it (WESS, WFAR, and WPOG) might possibly be affected by subduction-related strain. Thus we assume that the coupled segment west of Unimak can extend no farther east than the western end of Unimak. *Johnson and Satake* [1997] modeled the 1946 earthquake as resulting from slip directly offshore of Unimak Island, where we infer free slip. This suggests that much of the source zone of the 1946 earthquake is weakly coupled, but we must consider the possibility that the megathrust offshore of westernmost Unimak Island might be strongly coupled.

[18] In our model for the subduction zone, we hold the location, strike, dip, slip and depth of the megathrust fault plane fixed. The values used are based on bathymetric maps, earthquake focal mechanisms from the Harvard centroid moment tensor (CMT) catalog (http://www.seismology.harvard.edu/projects/CMT), and the revised NUVEL-1A plate motion between the Pacific and the North American plates [*DeMets and Dixon*, 1999]. The strike and dip of the fault plane are N56°E and 21°, respectively, and the depth of the updip end of the locked zone at the trench is 7 km. The plate velocity is 66.8 mm yr^{-1} and true trench normal. The two additional model parameters we estimate are the width of the locked interface and the degree of interseismic coupling. The degree of coupling is defined as the ratio of the virtual slip rate to the relative plate speed [*Savage*, 1983]. Zero coupling implies free slip. The estimated values for the volcanic sources are very similar to the first model run, and are summarized in Tables 2 and 3, respectively.

[19] In the best fit model, the estimated width of the locked zone is 65 km, and the degree of coupling is 30%. With an average dip of 21° this would lead to a maximum depth of 30 km for the lower end of the locked zone. This narrow zone of weak coupling results from the lack of obvious contraction in the direction of plate motion. A zone of weak coupling helps to explain the deflection of the SCAP velocity from the radial pattern but must be small enough not to change the velocities of the other sites. Fitting our whole GPS data set (36 observations) with just volcanic sources gives an SSE of 33.60. Adding two parameters for the subduction component reduces the SSE slightly to 32.56. This improvement is not statistically significant at the 95% confidence level, based on an F test.

4. Model Interpretation and Discussion

4.1. Inflation of Westdahl

[20] The GPS data show inflation of Westdahl volcano between 1998 and 2001. This inflation has continued since at least 1993, as shown by SAR interferometry [*Lu et al.*, 2000a]. Compared with the InSAR results, which span the earlier time period between 1993 and 1998, the rate of inflation from 1998 to 2001 might have decreased slightly. The calculated volume change rate is only ~70% of that

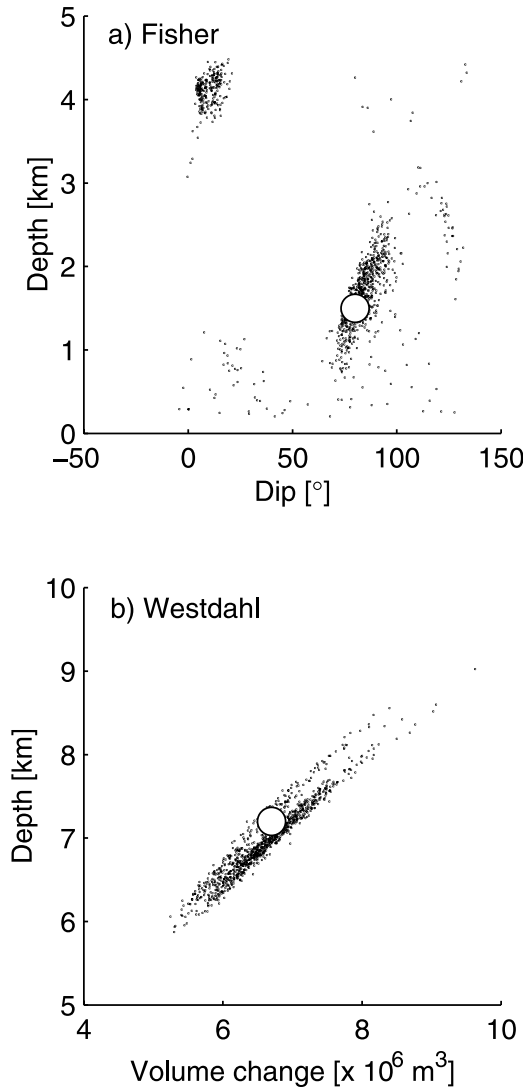

Figure 4. Correlation between (a) depth and dip for a rectangular dislocation source in Fisher caldera and (b) the depth and subsurface volume change for a point source beneath Westdahl. Each dot indicates the best fit pair of one bootstrap model. The open circle indicates the overall best fit model. Figure 4a shows that depth and dip of the dislocation source are bimodally distributed, allowing either a shallow and vertical, or deeper and horizontal geometry. Figure 4b shows the trade-off between source depth and volume change. Models with a shallow depth and low volume change give a similar good data fit as models with greater depth and higher volume change.

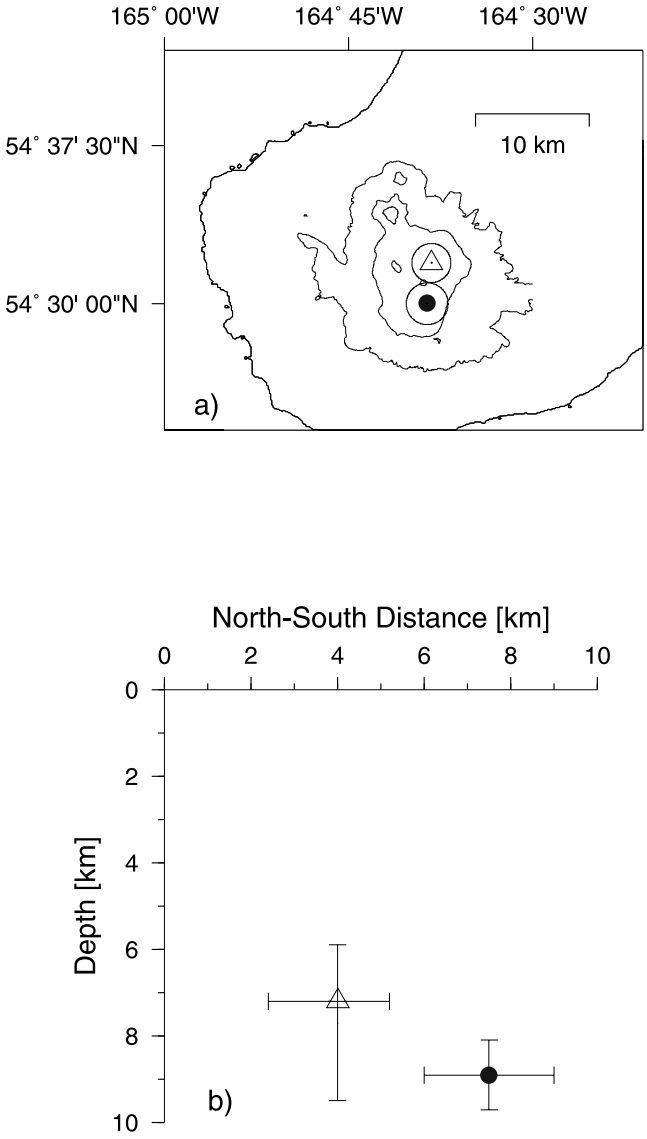

Figure 5. Comparison of GPS (triangle) and InSAR (solid circle) modeling results for location and depth of the inflation source underneath Westdahl volcano. GPS models are based on data between 1998 and 2001, InSAR models are based on data between 1993 and 1998 [*Lu et al.*, 2000a]. Uncertainties show 95% confidence. (a) Source location in map view. (b) Source location and depth along a north–south profile. Uncertainty ranges for the depth overlap in GPS and InSAR models, while they are slightly separated in north–south location.

derived from InSAR, and the source depth is shallower by 1.7 km. Both depth and volume change are within uncertainties of GPS and InSAR modeling, however, and the difference could be explained by the trade-off between source depth and strength (Figure 4b). This means that a shallower source could produce a deformation pattern that is indistinguishable from a deeper and stronger one, given the current network geometry and data precision.

[21] The GPS model places the source location 3.5 km farther north than the InSAR model. This is slightly outside the uncertainty range and may indicate a true movement of the source. A comparison between GPS and InSAR modeling results for source location and depth is shown in Figure 5.

[22] From these deformation observations alone it is difficult to judge whether activity at Westdahl is generally decreasing or actively building toward a new eruption. Possible indicators for an impending eruption at Westdahl would be an increase in deformation rate, movement of the source to significantly shallower levels, or an increase in seismicity. We do not know at what timescales these precursors would occur, but we do have additional information from seismicity and mass balance calculations about the state of the system. Deformation at Westdahl is occurring aseismically, with only very few (<5) high- or low-frequency events detected since installation of the seismic network in 1998. This suggests that magma has not moved to shallower, more brittle levels of the crust, and thus the deformation is resulting from a relatively stable source at depth. No seismic records exist prior to the 1991/1992 eruption, and so it may require a new eruption to learn whether there are long-term seismic precursors or if the aseismic behavior is typical for activity at Westdahl.

[23] The total subsurface volume increase during the InSAR and GPS observation period (1993–2001) is $\sim 70 \times 10^6$ m^3. Treating magma as an incompressible fluid, this would be equal to the volume of accumulated new magma. If we consider bulk compression of resident magma by newly injected magma, the accumulated magma volume could exceed this value by ~50% [*Johnson et al.*, 2000]. Thus the magma accumulation between 1993 and 2001 exceeds the $30-60 \times 10^6$ m^3 erupted during the last eruption in 1991/1992 [*Rowland et al.*, 1994]. This suggests that the magma refilling process may be completed and/or that the pressure in the system is increasing. This is neither a necessary nor a sufficient condition for a new volcanic eruption, but it is compelling evidence that the magmatic system is highly active.

4.2. Subsidence and Contraction of Fisher Caldera

[24] Most historical unrest at large calderas is caused by a combination of local magmatic, tectonic, or hydrologic processes [*Newhall and Dzurisin*, 1988]. We examine the following mechanisms to explain the subsidence and contraction of Fisher caldera: removal and migration of magmatic or hydrothermal fluids, magma crystallization and thermal contraction, and depressurization of the hydrothermal reservoir. There is no indication of tectonic causes, like regional crustal extension, for caldera subsidence.

4.2.1. Removal and Migration of Magmatic or Hydrothermal Fluids

[25] The volume decrease rate inferred from the dislocation model is 2.0×10^6 m^3 yr^{-1} between 1999 and 2001. No magma extruded during this time, and there is no evidence for uplift caused by shallow intrusions or migration of fluids with in the caldera, as observed in Yellowstone caldera over similar times cales [*Wicks et al.*, 1998]. All GPS sites inside Fisher caldera are subsiding. We cannot completely rule out the possibility of intracaldera migration, however, because too few sites were surveyed precisely every year to resolve variations within the 2-year observation period.

[26] Areas of uplift do exist at greater distances from the caldera. Westdahl volcano, 20 km to the southwest, has

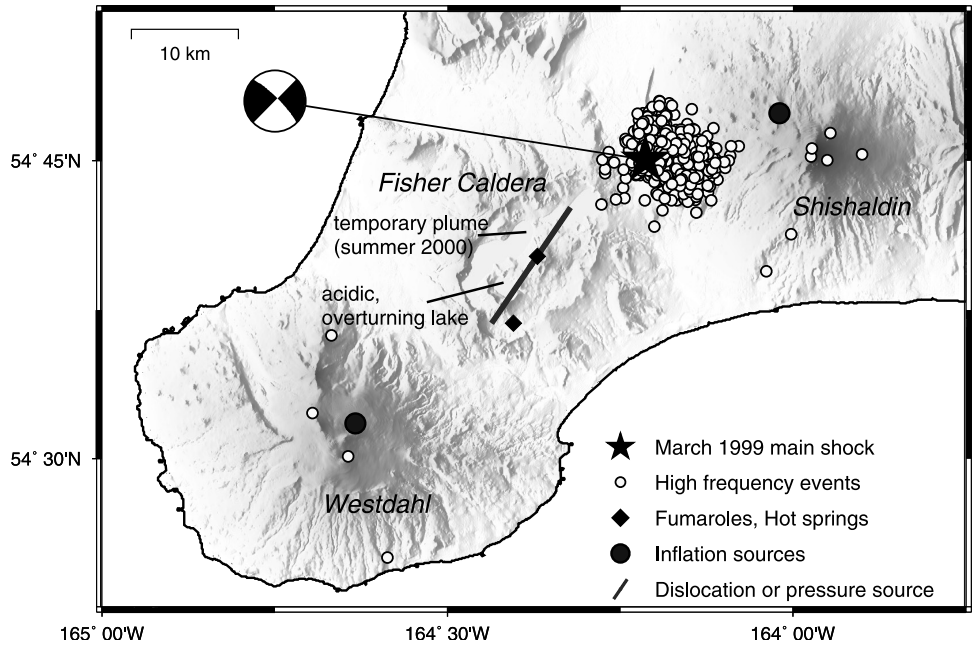

Figure 6. Summary of volcanic, hydrothermal, and tectonic activity on Unimak Island. Westdahl has been inflating since the last eruption in 1991–1992. Shishaldin erupted in April 1999 and shows localized inflation on the northwest flank. Fisher caldera's hydrothermal system is expressed through fumaroles, hot springs, an acidic, actively overturning lake, and a temporary plume in one of its other lakes, which was observed during the summer of 2000. Earthquakes shown are detected high-frequency events between July 1998 and July 2001, the period of the GPS survey. The M 5 earthquake occurred on 4 March 1999. Events in that area declined in number but continued throughout the GPS survey period. Notice the absence of significant seismicity accompanying inflation of Westdahl. Data are from the Alaska Volcano Observatory seismic network.

been inflating during that time, as discussed above. Shishaldin volcano, 20 km to the northeast, shows local inflation northwest of the central cone [*Masterlark et al.*, 2001; D. Mann, unpublished data, 2001] (Figure 6). It seems unlikely, however, that magma from a shallow (2 km) reservoir at Fisher would move back down to a much deeper (7 km) reservoir at Westdahl. There is no evidence from the GPS data that would indicate this intrusion. In the area between Fisher and Shishaldin we have little control from the geodetic data, and could have missed an intrusion. Current evidence based on isotopic $\delta^{18}O$ data for Fisher tephras shows, however, that the magmatic systems of the Unimak island volcanoes are not connected [*Bindeman et al.*, 2001]). Thus migration of magma from the chamber below Fisher to Westdahl or Shishaldin seems unlikely.

4.2.2. Magma Crystallization and Thermal Contraction

[27] The active hydrothermal system, the acidic overturning lake, plumes in one of the other intracaldera lakes (Figure 6), and the occasional strong sulfur smell are all strong evidence for a magmatic heat source beneath Fisher. Our best fit deformation model has the geometry of a shallow dike or somewhat deeper sill, with a contraction rate of $\sim$0.3 m yr^{-1}, if all of the deformation is to be explained by volume rather than pressure change. We will assume here that it represents a dike. Such a dike may have been intruded any time before the start of our observations in the summer of 1999. The observed subsidence and contraction could then result from contractional cooling and gas release during crystallization.

[28] The thermal contraction of such a dike is given by

$$\frac{\Delta V}{V} = \alpha_v \Delta T, \tag{1}$$

where ΔV is the resulting volume change, V is the total volume of the dike, α_v the volumetric coefficient of thermal expansion, and ΔT the temperature drop due to cooling. The total volume and temperature drop are both unknown. α_v is on the order of $\sim 10^{-4}$ K^{-1} for silicate melt and $\sim 3 \times 10^{-5}$ K^{-1} for typical minerals of crystallizing magma [*Williams and McBirney*, 1979]. With an average estimate of $\alpha_v = 10^{-5}$ K^{-1}, the modeled total volume decrease, $\Delta V = 4.0 \times 10^6$ m^3, and an area of the dike (length times width, see Table 3) of 7×10^6 m^2, we obtain $h\Delta T$ = 57,000 [m K], with h being the thickness of the dike in meters. Even with the maximum plausible amount of cooling, the result of this calculation would imply a giant dike on the order of tens to hundreds of meters thick (Figure 7a). It is unlikely that a shallow dike emplacement of this size would have gone unnoticed any time within the last few decades, even without seismometers in place locally. On Akutan Island, 150 km to the southwest of Unimak, the intrusion of a 2.5 m thick dike at 0.5 km depth was accompanied by an intense earthquake swarm that was felt widely across the island and recorded teleseismically [*Lu et al.*, 2000b].

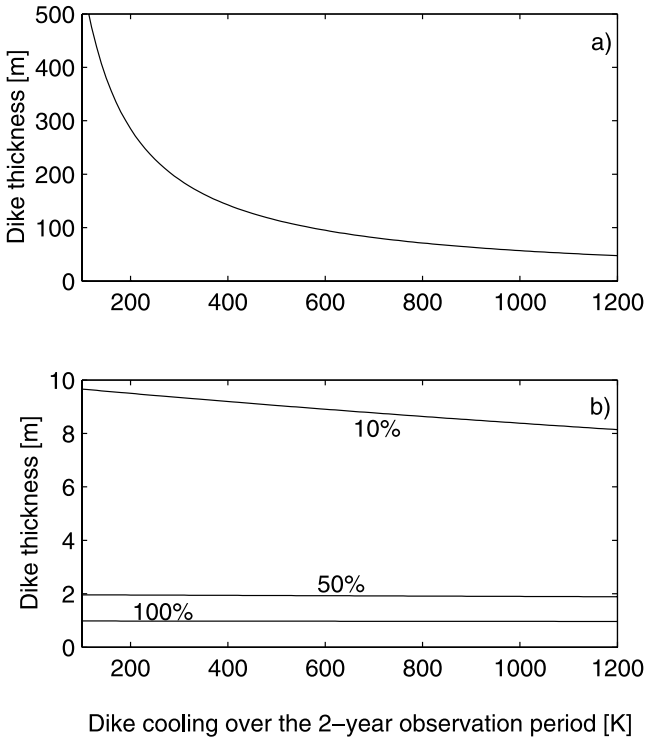

Figure 7. Dike thickness as a function of cooling rate if deformation is caused by (a) contractional cooling alone or (b) contractional cooling plus degassing of the magma. Contractional cooling alone would require a giant dike even at the highest possible cooling rates. If part of the volume loss is caused by degassing of the magma, the required dike thickness reduces to 1.0 to 10 m. Curves represent degassing of 10%, 50%, and 100% of a melt with originally 3 wt % H_2O at a pressure of 45 MPa.

[29] An additional source of volume loss could be gas release during crystallization, which is another consequence of the cooling process. Assuming that the main gas released is water vapor, the maximum volume loss due to this process is given by

$$\frac{\Delta V}{V} = \frac{m_g}{m_b}\frac{\rho_b}{\rho_g}, \tag{2}$$

where m is the mass, ρ is the density, and the indices g and b denote gas and bulk magma properties, respectively. We calculate the volume ratio for a basaltic melt with originally 3 wt % water at a pressure of 45 MPa (corresponding to 1.6 km depth), and at a temperature of 1100°C. Using the relations described by *Philpotts* [1990], we find that ~55% of the original dike volume could be released as water vapor if all water was lost. This implies a minimum dike thickness of 1 m to account for the total volume loss we observed. A dike of this thickness, however, would solidify within ~2 weeks, meaning that it would be required to have been emplaced just prior to when our observations started.

[30] It seems unlikely that we timed our first survey right after the intrusion of a 1-m-thick dike and captured the short time period of solidification and complete degassing, which would also imply that most of the deformation observed occurred within days after the first survey.

[31] If only part of the gas was released during crystallization, the required dike thickness increases accordingly (Figure 7b), resulting in a longer solidification time and extending the possible time period in which emplacement could have occurred. If we assume a sill geometry, then a thicker (and less crystallized) sill is more plausible than a very thick dike. Cooling times for a sill would be slightly increased, extending the possible emplacement time period even further.

[32] It thus appears most likely that deformation has been caused by a partly degassed dike or sill. Such a dike or sill could have been emplaced in conjunction with seismic activity between Fisher and Shishaldin starting in March 1999 (Figure 6), 4 months before the first survey in Fisher caldera. A dike or sill between 8 and 18 m thick that then solidified during the GPS survey period from July 1999 to July 2001 and lost ~10% of its original gas volume, would be in agreement with the GPS data, but the size of this dike or sill requires us to consider alternate mechanisms to explain the observed deformation.

4.2.3. Depressurization of the Hydrothermal Reservoir

[33] The fact that the location of our best fit sources, both the dislocation source and the ellipsoidal pressure source, coincide with the areas of highest hydrothermal activity (Figure 6), suggests a close connection between deformation and changes in the hydrothermal system. Depressurization could be the current state in a system of cyclic increase and release of pressure. In this model, increase of pressure is caused by trapping of fluids and gases beneath an impermeable layer, possibly created by crystallization of an underlying magma body, and decrease of pressure follows when the impermeable layer ruptures and fluids and gases escape [*Dzurisin et al.*, 1994]. The existence of such a self-sealed layer is reported from several hydrothermal systems in calderas, like Yellowstone and Campi Flegrei [*Dvorak and Dzurisin*, 1997]. Rupture of this layer might be triggered by a nearby earthquake.

[34] The history of recorded seismicity on Unimak island is relatively short, starting with the installation of a seismic network around Shishaldin by the Alaska Volcano Observatory in 1997. The main seismic activity since then was a shallow earthquake sequence with an M_L 5 main shock, located ~10 km NE of Fisher and 14 km west of Shishaldin, that occurred in March 1999. Prior to this, no shallow earthquake $M > 4.5$ has been located in the vicinity of Fisher since the start of the National Earthquake Information Center (NEIC) database in 1973. Therefore the 1999 event would be the most likely candidate for a trigger. The earthquake sequence was located outside of the caldera (Figure 6), but this is similar to events at Long Valley caldera in 1978–1980 [*Savage and Clark*, 1982; *Hill et al.*, 1985] and Yellowstone caldera in 1959 and 1985 [*Savage et al.*, 1993], where a connection between seismicity outside and deformation inside the respective calderas was detected. The 1985 earthquake swarm outside of Yellowstone caldera coincided with the onset of caldera subsidence after long-term uplift before 1984 and no detectable movement between 1984 and 1985 [*Dzurisin et al.*, 1994]. The 1999 Unimak earthquake occurred 6 weeks before Shishaldin erupted in April 1999. It is unlikely that this earthquake

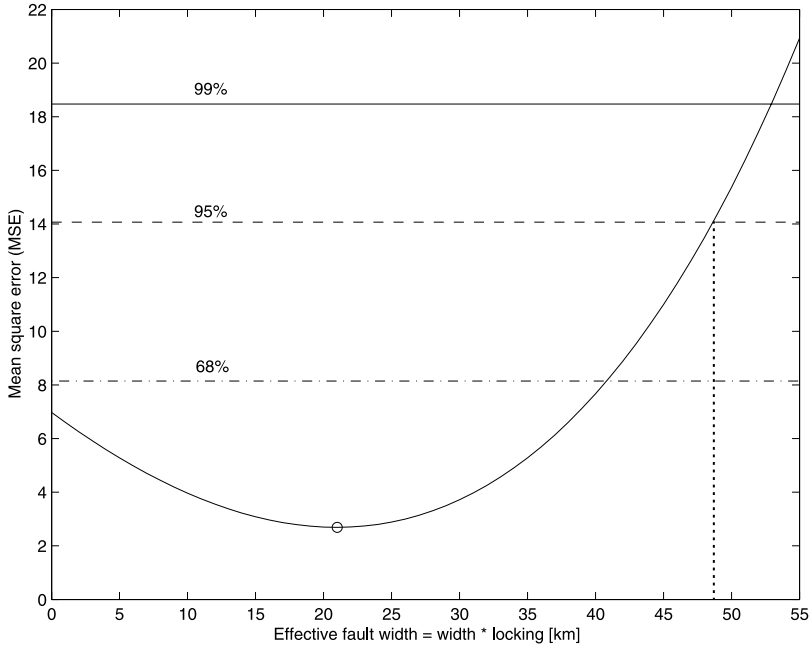

Figure 8. Mean square error (MSE) versus effective fault width (width times coupling) when all other model parameters are held fixed, and only data from SCAP, WESS, WFAR, and WPOG are included in the modeling. Horizontal lines limit 68% (dashed point), 95% (dashed), and 99% (solid) confidence regions based on the increase in misfit of these models. The vertical line determines the upper bound for the effective width to be 48 km within 95% confidence. The circle indicates the minimum misfit at an effective width of 21 km.

triggered the eruption, but it could have occurred as a direct result of a dike injection beneath Shishaldin [*Moran et al.*, 2002]. In this scenario, activity at Shishaldin would have caused changes in Fisher's hydrothermal system without any magma exchange.

[35] To assess the depressurization process quantitatively, we modeled the deformation using a finite ellipsoidal pressure source instead of a dislocation model. We estimate an average pressure decrease of 25 kPa yr^{-1}. Assuming that this pressure decrease is caused by the release of gas, we use the ideal gas equation

$$PV = nRT, \tag{3}$$

where P is the pressure, V is the volume, n is the number of moles, R is the universal gas constant, and T is the temperature, to calculate the amount of gas released. We set P and V equal to the results from the deformation modeling, the pressure release and the volume of the ellipsoid, respectively. T is assumed to be 100°C, as an average fumarolic temperature. No detailed gas chemistry analysis has been conducted for Fisher caldera, but the typical composition of gases emitted from fumaroles associated with volcanic vents in the Aleutians is ~99 mol % H_2O, 0.8 mol % CO_2, and 0.2 mol % SO_2 and H_2S [*Motyka et al.*, 1993]. Using this composition, we find that ~640 kt yr^{-1} H_2O, ~13 kt yr^{-1} CO_2, and ~4 kt yr^{-1} SO_2 and H_2S combined would be released. Compared with similar systems, these are typical background levels, and about one order of magnitude smaller than the tree-killing CO_2 emissions at Mammoth Mountain [*Farrar et al.*, 1995], and ~2 orders of magnitude smaller than emissions during excessive degassing at other volcanic system, e.g., Izu-Oshima between 1988 and 1990 [*Kazahaya et al.*, 1994]. In situ measurements of actual gas emissions and comparison with the predicted values would be necessary to evaluate the contribution of hydrothermal depressurization, caused by release of formerly trapped gases after rupturing a seal, to the observed subsidence.

4.3. No Significant Strain Accumulation Across Unimak Island

[36] The interseismic degree of coupling at the subduction interface at the western end of Unimak Island is difficult to determine but is clearly low. This result is somewhat surprising, given the earthquake history of the region. Figure 8 shows the mean square error (MSE) versus the effective locked fault width (defined as fault width times the degree of coupling) when all volcanic source parameters are held fixed at the best fit model values. Within the 95% confidence range, the upper bound for the effective width of a locked zone starting at the trench is 48 km. The best estimate for the effective locked width is 20 km.

[37] If we assume that the lower end of a locked zone is not deeper than 35 km, a typical figure for the bottom of the seismogenic zone [*Tichelaar and Ruff*, 1993], the width should be less than 80 km for geometric reasons. This constrains the maximum allowable degree of coupling to 60%. In this case, as well as in the best fit model obtained from modeling width and coupling as independent parameters (65 km width, 30% coupled), the 1957 aftershock zone would not be part of the locked area, because it is located at greater depth. Any locked patch within the 1946 rupture zone must be either weakly coupled or small, or both.

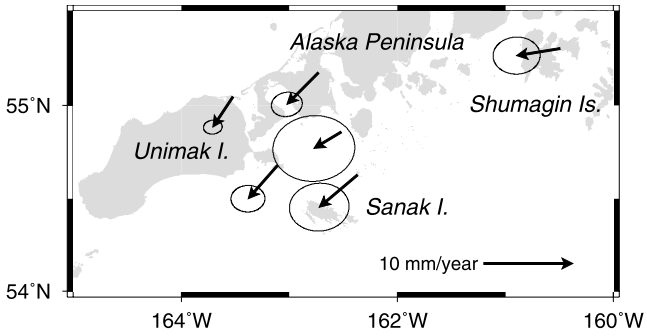

Figure 9. Velocities of selected GPS sites on Unimak and Sanak Islands, the Shumagins, and the Alaska Peninsula relative to North America. Error ellipses indicate 95% confidence regions. All sites show displacement of ~4 mm yr^{-1} to the southwest, slightly toward the trench. Data from additional sites are shown by *Freymueller and Beavan* [1999].

Zweck et al. [2002] suggested that the locked patches observed with GPS geodesy are in fact the asperities that ruptured in the last earthquake cycle; based on this interpretation, we infer that if an asperity is present in the 1946 earthquake source region, it must be small.

[38] It is important to note that at the 95% confidence level, a completely locked zone of up to 48 km width cannot be distinguished from a completely unlocked interface (Figure 8). This means that across the entire island no significant strain accumulation due to subduction is observed. Our results are contrary to what would be expected from an 80–100 km wide asperity capable of slipping 10 m in an earthquake. In deriving this upper bound, we have assumed that the megathrust is locked and thus seismogenic all the way out to the trench, a assumption similar to that of *Johnson and Satake* [1997]. If, instead, the updip limit of the locked zone is some distance inboard of the trench, as is often assumed, the maximum allowable locked zone shrinks because we can only allow a locked region small enough not to cause a significant observed deformation signal. The upper bound on the allowable locked zone would shrink substantially with more precise GPS data, particularly for the sites on the south side of Westdahl.

[39] It is plausible that a fully locked zone 20 km wide and 80–100 km long could generate an M_S 7.4 earthquake, but slip over such a limited area cannot explain the giant 1946 tsunami [*Johnson and Satake*, 1997]. Thus the absence of strain due to the megathrust is a powerful argument in favor of a landslide source for the 1946 earthquake and tsunami. The GPS data are not violated by the presence of a relatively small asperity located close to the trench. In the scenario outlined by *Fryer et al.* [2002], rupture of such an asperity in an earthquake of M_S 7.4 or smaller would then have triggered a large landslide, generating the huge tsunami. *Fryer et al.* [2002] showed evidence for several large submarine landslides offshore of Unimak Island and the eastern Aleutian arc. One of these landslides is located in the right place to be the cause of the 1946 tsunami (G. Fryer, personal communication, 2002). Although none of these features have been sampled, and thus their dates are unknown, *Fryer et al.* [2002] suggested that such landslides have been fairly common (over geologic time).

4.4. Translation of the Alaska Peninsula and Unimak Island

[40] Relative to North America, station KATY as well as other sites along the Alaska Peninsula immediately to the east move consistently at ~4 mm yr^{-1}, with a direction oriented slightly more southerly than trench parallel or slightly toward the trench (Figure 9). *Freymueller and Beavan* [1999] found that the only component of the strain tensor that was marginally significant was a trench-parallel extension that was not significantly different from zero at the two sigma level. The velocities of those sites relative to North America agree with the direction of maximum extension. Because there is no sign of strain associated with the subduction earthquake cycle, we interpret these velocities to indicate southwestward translation of this portion of the Alaska Peninsula relative to North America. Data from sites further to the northeast suggest that the entire Alaska Peninsula may move at about the same rate. *Fletcher et al.* [2001] found a significant trench-parallel component of ~5 mm yr^{-1} in velocities of sites in the Semidi Islands, 200 km SW of Kodiak Island and 400 km NE of Unimak. VLBI data from Sand Point in the Shumagin Islands also showed a significant trench-parallel component of velocity [*Ma et al.*, 1990], which was mysterious at the time.

[41] This southwestward translation of a large section of the Alaska Peninsula and Aleutian Arc, including Unimak Island, relative to North America, could result from any of three different mechanisms: (1) motion of the Bering Sea microplate [*Mackey et al.*, 1997]; (2) translation of a large section of southern Alaska on the Denali fault system [*Fletcher*, 2002]; or (3) translation of a forearc/arc sliver resulting from oblique subduction [e.g., *McCaffrey*, 1992]. Farther to the west, *Ave Lallemant and Oldow* [2000] presented GPS data that shows westward translation of much of the Aleutian arc, which increases from a few millimeters per year at Dutch Harbor (located 200 km southwest of Unimak) to as much as 30 mm yr^{-1} at Attu in the Western Aleutians.

5. Conclusions

[42] GPS data acquired between 1998 and 2001 show active deformation of two of the volcanoes on Unimak Island, Westdahl, and Fisher. Westdahl has been continuously inflating since its last eruption in 1991/1992, with a source at 7.2 km depth beneath the surface. Mass balance calculations show that more new magma has already accumulated since 1993 than was previously erupted in 1991/1992. No seismic activity has been reported, and during the three years of the GPS campaign inflation has been completely aseismic.

[43] Contraction and subsidence in Fisher caldera cannot be related to any eruptive activity. It is best explained by degassing and thermal contraction of a shallow crystallizing magma body or depressurization of Fisher's hydrothermal system. In either case, a recent intrusion beneath Fisher is required. Future measurements may help to identify the dominant process. In the case of cyclic changes of the hydrothermal system as cause for the deformation,

the rate of contraction should not only decrease with time as the system reequilibrates but eventually reverse into inflation.

[44] In a regional tectonic framework, the GPS data show that at the 95% confidence level there is no significant strain accumulation due to subduction across Unimak Island. The only evidence for subduction-related deformation is at the western end of the island, but the coupling of the plate interfaces is either low or limited to a width of 48 km or less. The lack of strain observed within the region of the 1946 tsunami earthquake is contrary to what would be expected if there was a large locked patch on the megathrust capable of generating the 1946 tsunami and is strong evidence in favor of a landslide source for that earthquake and tsunami. Relative to North America, stations on Unimak move SW-ward, following a trend observed by other workers along large sections of the Alaska Peninsula and Aleutian arc.

[45] **Acknowledgments.** This study was supported by NASA grant NAG5-7659. Funding for fieldwork and logistical support was mainly provided by the Alaska Volcano Observatory, and by a Jack Kleinman Grant for volcano research in 2000. Some field equipment was borrowed from UNAVCO. Alaska Maritime National Wildlife Refuge and the Isanotski Corporation permitted access to the field sites. We would like to thank Chuck Martinson at Peter Pan Seafoods in False Pass for many occasions of unconventional help during the fieldwork. Bill Springer of Maritime Helicopters was an excellent pilot and navigator in sometimes very difficult flying conditions. We thank Jim Gardner, Chris Nye, and Pete Stelling for helpful discussions and insightful comments on this manuscript and many other aspects of volcanic activity on Unimak Island and in the Aleutians. Comments by P. Cervelli and two anonymous reviewers improved the manuscript.

References

Abe, K., Size of great earthquakes of 1873–1974 inferred from tsunami data, *J. Geophys. Res.*, *84*, 1561–1568, 1979.

Ave Lallemant, H. G., and J. Oldow, Active displacement partitioning and arc-parallel extension of the Aleutian volcanic arc based on Global Positioning System geodesy and kinematic analysis, *Geology*, *28*, 739–742, 2000.

Berg, B., Locating global minima in optimization problems by a random-cost approach, *Nature*, *361*, 708–710, 1993.

Bindeman, I. N., J. H. Fournelle, and J. W. Valley, Low-$\delta^{18}O$ tephra from a compositionally zoned magma body: Fisher Caldera, Unimak Island, Aleutians, *J. Volcanol. Geotherm. Res.*, *111*, 35–53, 2001.

Boucher, C., Z. Altamimi, and P. Sillard, The 1997 International Terrestrial Reference Frame (ITRF97), in *IERS Tech. Note 27*, Obs. de Paris, Paris, 1999.

Cervelli, P., M. H. Murray, P. Segall, Y. Aoki, and T. Kato, Estimating source parameters from deformation data, with an application to the March 1997 earthquake swarm off the Izu Peninsula, Japan, *J. Geophys. Res.*, *106*, 11,217–11,237, 2001.

Davies, J., L. Sykes, L. House, and K. Jacob, Shumagin seismic gap, Alaska peninsula: History of great earthquakes, tectonic setting, and evidence for high seismic potential, *J. Geophys. Res.*, *86*, 3821–3855, 1981.

DeMets, C., and T. H. Dixon, New kinematic models for Pacific-North American motion from 3 Ma to present, I: Evidence for steady state motion and biases in the NUVEL-1A model, *Geophys. Res. Lett.*, *26*, 1921–1924, 1999.

Dvorak, J. J., and D. Dzurisin, Volcano geodesy: The search for magma reservoirs and the formation of eruptive vents, *Rev. Geophys.*, *35*, 343–384, 1997.

Dzurisin, D., K. M. Yamashita, and J. W. Kleinman, Mechanisms of crustal uplift and subsidence at the Yellowstone caldera, Wyoming, *Bull. Volcanol.*, *56*, 261–270, 1994.

Farrar, C. D., M. L. Sorey, W. C. Evans, J. F. Howle, B. D. Kerr, B. M. Kennedy, C.-Y King, and J. R. Southon, Forest-killing diffuse CO_2 emission at Mammoth Mountain as a sign of magmatic unrest, *Nature*, *376*, 675–678, 1995.

Fletcher, H. J., Crustal deformation in Alaska measured using the Global Positioning System, Ph.D. thesis, Univ. of Alaska, Fairbanks, 2002.

Fletcher, H. J., J. Beavan, J. T. Freymueller, and L. Gilbert, High interseismic coupling of the Alaska subduction zone SW of Kodiak Island inferred from GPS data, *Geophys. Res. Lett.*, *28*, 443–446, 2001.

Freymueller, J. T., and J. Beavan, Absence of strain accumulation in the Western Shumagin segment of the Alaska subduction zone, *Geophys. Res. Lett.*, *26*, 3233–3236, 1999.

Freymueller, J. T., M. H. Murray, P. Segall, and D. Castillo, Kinematics of the Pacific-North America plate boundary zone, northern California, *J. Geophys. Res.*, *104*, 7419–7441, 1999.

Freymueller, J. T., S. C. Cohen, and H. J. Fletcher, Spatial variations in present-day deformation, Kenai Peninsula, Alaska, and their implications, *J. Geophys. Res.*, *105*, 8079–8101, 1999.

Fryer, G. J., P. Watts, and L. F. Pratson, Source of the great tsunami of 1 April 1946: A landslide in the upper Aleutian forearc, *Mar. Geol*, submitted, 2002.

Hill, D. P., R. A. Bailey, and A. S. Ryall, Active tectonic and magmatic processes beneath Long Valley caldera, eastern California: A summary, *J. Geophys. Res.*, *90*, 11,111–11,120, 1985.

Johnson, D. J., F. Sigmundsson, and P. T. Delaney, Comment on "Volume of magma accumulation or withdrawal estimated from surface uplift or subsidence, with application to the 1960 collapse of Kilauea volcano" by P. T. Delaney and D. F. McTigue, *Bull. Volcanol.*, *61*, 491–493, 2000.

Johnson, J. M., and K. Satake, Source parameters of the 1957 Aleutian Earthquake from tsunami waveforms, *Geophys. Res. Lett.*, *20*, 1487–1490, 1993.

Johnson, J. M., and K. Satake, Estimation of seismic moment and slip distribution of the April 1, 1946, Aleutian tsunami earthquake, *J. Geophys. Res.*, *102*, 11,765–11,774, 1997.

Johnson, J. M., K. Satake, S. R. Holdahl, and J. Sauber, The 1964 Prince William Sound earthquake: Joint inversion of tsunami and geodetic data, *J. Geophys. Res.*, *101*, 523–532, 1996.

Kanamori, H., The energy release in great earthquakes, *J. Geophys. Res.*, *82*, 2981–2987, 1977.

Kanamori, H., Non-double-couple seismic source, paper presented at XXIIrd General Assembly, Int. Assoc. of Seismol. and Phys. of Earth Inter., Tokyo, Japan, 1985.

Kazahaya, K., H. Shinohara, and G. Saito, Excessive degassing of Izu-Oshima volcano: Magma convection in a conduit, *Bull. Volcanol.*, *56*, 207–216, 1994.

Lu, Z., C. Wicks, D. Dzurisin, W. Thatcher, J. T. Freymueller, S. R. McNutt, and D. Mann, Aseismic inflation of Westdahl volcano, Alaska, revealed by satellite radar interferometry, *Geophys. Res. Lett.*, *27*, 1567–1570, 2000a.

Lu, Z., C. Wicks, J. A. Power, and D. Dzurisin, Ground deformation associated with the March 1996 earthquake swarm at Akutan volcano, Alaska, revealed by satellite radar interferometry, *J. Geophys. Res.*, *105*, 21,483–21,495, 2000b.

Ma, C., J. M. Sauber, L. J. Bell, T. A. Clark, D. Gordon, W. E. Himwich, and J. W. Ryan, Measurement of horizontal motions in Alaska using very long baseline interferometry, *J. Geophys. Res.*, *95*, 21,991–22,011, 1990.

Mackey, K. G., K. Fujita, L. V. Gunbina, V. N. Kovalev, V. S. Imaev, B. M. Kozmin, and L. P. Imaeva, Seismicity of the Bering Strait region: Evidence for a rotating Bering Block, *Geology*, *25*, 979–982, 1997.

Masterlark, T., Z. Lu, S. C. Moran, and C. W. Wicks, Inflation rate of Shishaldin volcano inferred from two-way stress coupling, *Eos Trans. AGU*, *82*(47), Fall Meet. Suppl., Abstract S21B-0584, 2001.

McCaffrey, R., Oblique plate convergence, slip vectors, and forearc deformation, *J. Geophys. Res.*, *97*, 8905–8915, 1992.

Miller, T. P., R. G. McGimsey, D. H. Richter, J. R. Riehle, C. J. Nye, M. E. Yount, and J. A. Dumoulin, Catalog of the historically active volcanoes of Alaska, *U.S. Geol. Surv. Open File Rep., 98–582*, 1998.

Mogi, K., Relations between the eruptions of various volcanoes and the deformations of the ground surface around them, *Bull. Earthquake Res. Inst. Univ. Tokyo*, *36*, 99–134, 1958.

Moran, S. C., S. D. Stihler, and J. A. Power, A tectonic earthquake sequence preceding the April–May 1999 eruption of Shishaldin volcano, Alaska, *Bull. Volcanol.*, *64*, 520–524 DOI 10.1007/s00445-002-0226-1, 2002.

Motyka, R. J., S. A. Liss, C. J. Nye, and M. A. MoormanGeothermal Resources of the Aleutian Arc, *Professional Report*, *114*, 17 pp., State of Alaska Dep. of Nat. Res., Div. of Geol. and Geophys. Surv., Fairbanks, 1993.

Newhall, C. G., and D. Dzurisin, Historical unrest at large calderas of the world, *U.S. Geol. Surv. Bull., 1855*, 2 vols, 1108 pp., 1988.

Okada, Y., Surface deformation due to shear and tensile faults in a half-space, *Bull. Seismol. Soc. Am.*, *75*, 1135–1154, 1985.

Okal, E. A., Seismic parameters controlling far-field tsunami amplitudes: A review, *Nat. Hazards*, *1*, 67–96, 1988.

Pelayo, A. M., Earthquake source parameter inversion using body and surface waves: Applications to tsunami earthquakes and Scotia Sea seismotectonics, Ph.D. thesis, Washington Univ., St. Louis, Mo., 1990.

Philpotts, A. R., *Principles of Igneous and Metamorphic Petrology*, 498 pp., Prentice-Hall, Old Tappan, N. J., 1990.

Rowland, S. K., G. A. Smith, and P. J. Mouginis-Mark, Preliminary ERS-1 Observations of Alaskan and Aleutian Volcanoes, *Remote Sens. Environ.*, *48*, 358–369, 1994.

Savage, J. C., A dislocation model of strain accumulation and release at a subduction zone, *J. Geophys. Res.*, *88*, 4984–4996, 1983.

Savage, J. C., and M. M. Clark, Magmatic resurgence in Long Valley caldera, California: Possible cause of the 1980 Mammoth Lakes earthquakes, *Science*, *217*, 531–533, 1982.

Savage, J. C., M. Lisowski, W. H. Prescott, and A. M. Pitt, Deformation from 1973 to 1987 in the epicentral area of the 1959 Hebgen Lake, Montana, earthquake (M_S = 7.5), *J. Geophys. Res.*, *98*, 2145–2153, 1993.

Sella, G., T. H. Dixon, and A. Mao, REVEL: A model for recent plate velocities from space geodesy, *J. Geophys. Res.*, *107*(B4), 2081, 10.1029/2000JB000033, 2002.

Tichelaar, B. W., and L. J. Ruff, Depth of seismic coupling along subduction zones, *J. Geophys. Res.*, *98*, 2017–2037, 1993.

Wicks, C., W. Thatcher, and D. Dzurisin, Migration of fluids beneath Yellowstone caldera inferred from satellite radar interferometry, *Science*, *282*, 458–462, 1998.

Williams, H., and A. R. McBirney, *Volcanology*, 397 pp., W. H. Freeman, New York, 1979.

Yang, X.-M., P. M. Davis, and J. H. Dieterich, Deformation from inflation of a dipping finite prolate spheroid in an elastic half-space as a model for volcanic stressing, *J. Geophys. Res.*, *93*, 4249–4257, 1988.

Zumberge, J. F., M. B. Heflin, D. C. Jefferson, M. M. Watkins, and F. H. Webb, Precise point positioning for the efficient and robust analysis of GPS data from large networks, *J. Geophys. Res.*, *102*, 5005–5018, 1997.

Zweck, C., J. Freymueller, and S. C. Cohen, Three-dimensional elastic dislocation modeling of the postseismic response to the 1964 Alaska earthquake, *J. Geophys. Res.*, *107*(B4), 2064, 10.1029/2001JB000409, 2002.

J. Freymueller, Geophysical Institute, University of Alaska Fairbanks, P.O. Box 757320, Fairbanks, AK 99775-7320, USA. (jeff@giseis.alaska.edu)

D. Mann, Department of Geophysics, Stanford University, 397 Panama Mall, Stanford, CA 94305, USA. (doerte@pangea.stanford.edu)